ON THE ERUPTIVE PHASE OF PROTON FLARES

E. I. MOGILEVSKII and V. N. ISHKOV

Institute of Terrestrial Magnetism, Ionosphere and Radiowave Propagation of the USSR Academy of Sciences

Abstract: The time development of the flare phenomena is analysed on the basis of the detailed cinephotography of the proton flare of 4th August, 1972 carried out with the IZMIRAN tower telescope using an "Opton" — 0.25 Å H_α filter with the shift of band along the Hα-contour, the observations of magnetic fields and radio emission. Special attention is paid to the development of eruptive phenomena: AFFS-systems, oscillating disturbances of a filament; prolonged ejections, and AFS. The estimate of the energy of eruptive phenomena in a flare, according to the measurements of filtergrams, shows that their energy is either comparable or even greater than the emission phase energy. Contrary to the emission phenomena, the eruptive phase energy is generated for a long period of time (over several hours of flare duration). A possible model representation of the AFFS-phenomena is given. The analysis of the totality of all flare-born phenomena shows that the eruptive phenomena establish a characteristic phase of the flare with which the generation and escape of corpuscular (SCR, SCF) geoeffective radiation are probably associated.

Measurements made by space vehicles show that practically during all flares (especially during strong ones) solar cosmic rays (SCR), a geoeffective wave emission and solar corpuscular fluxes (SCF) are generated. Of a peculiar interest are the proton flares as the most intense phenomena during which some emission and dynamic displays of flares are shown most expressively. From this point of view, the active period of 28 July — 12 August, 1972 (in particular, the very intense proton flare of 4th August) is of great interest. During this period many observational data were obtained on the dynamics and structure of chromospheric phenomena at IZMIRAN, and the development of the 4th August flare was cinephotographed in detail. With a relatively good stability of the image (there were many vibrations of $1 \div 2''$) of the tower telescope (diameter of solar image $D = 168$ mm) the recording was made with the help of a norrow-band ($\Delta\lambda = 0.25$ Å) IPF-H_α "Opton" with a discrete shift of band all over the contour of the line. This made it possible to watch the variation of the line-of-sight velocity field and motions along the surface at different chromospheric altitudes of the active region (A. R.). In the presence of A. R. magnetic charts, the filtergrams taken all over the contour of the H_α-line give especially valuable information on the dynamics of the chromospheric phenomena in the flare. Below we shall elucidate mainly this part of the proton flare development.

The present paper is to be considered only as the first step in the phenomenological analysis of our observational data. Information about the observations made at IZMIRAN and their preliminary analysis is given in the paper by Mogilevskii (1973), and these data are compared with the radio astronomical observations of the 4th August flare in the paper by Akinyan et al. (1973).

Observational Material

Observations were made by the IZMIRAN tower telescope. The IPF-H_α "Opton" with the cinecamera (frame size $165 \times 240''$) was placed near the focal plane of the Newton focus. As can be seen from Fig. 1, the high-quality filtergrams had a resolution not worse than $1 \div 2''$. At the end of the flare recording the atmospheric conditions became unstable, however most of the filtergrams are of a rather good quality. Every 30 s the total series of filtergrams was repeated with a step of 0.2 Å over the whole contour (± 0.8 Å). As regards ejections, in some series the band was shifted up to $1.5 \div 2.5$ Å. At each point of the contour a group of frames was obtained ($3 \div 10$)

which allowed us to choose the best ones for treatment. Due to a large diapason of brightness (details of the flare and the chromospheric fine structure) and the change of this relation of intensities, with the shift of band along the contour, in a number of filtergrams not all the elements of the

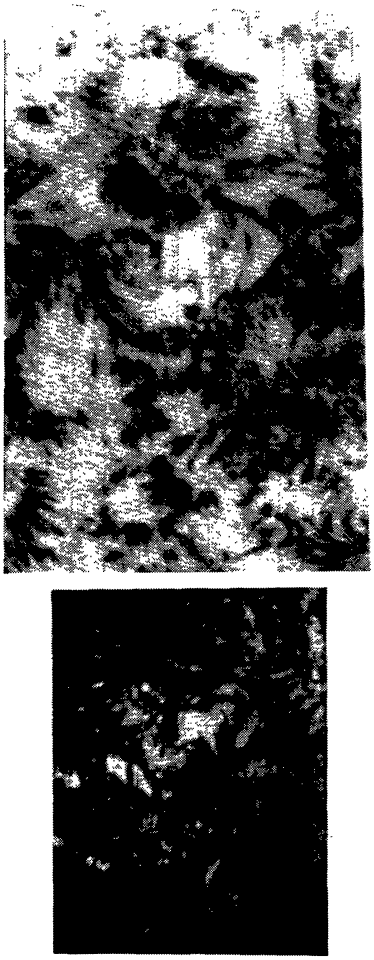

Fig. 1. (a) Example of H_α-filtergram of A. R. and corresponding (reduced scale) Dopplerogram by the Leighton method (b).The latter is obtained by the method of photographic subtraction (with $\gamma = 1$) of filtergrams taken at symmetrical points of the H_α-contour. Light spots correspond to motion away from the observer, dark ones – towards the observer.

flare could be photometered. However, most of the filtergrams can be photometred and the field of velocities determined, which is the basis of our work. In future we intend to use more effective techniques of qualitative analysis of the obtained data (Dopplerograms, statistical analysis with coherent and incoherent rays, etc.). Only a small part of the obtained material is used in the present work.

Development of A. R. and the Flare of 4th August

In spite of an extreme intensity, the flare of 4th August (the same as A. R. with the group N 223 (331) is largely a typical phenomenon.* The compactness of the structure and the magnetic field of the spot of the "δ"-configuration with the presence of very large field gradients considerable changes of the number and site of umbrae (in particular of the small ones), the splitting and diffusion of pore chains and small portions of the penumbra — these are the external peculiarities of the group. In this respect it resembles the group of the previous solar cycle N 379, 1959 ($\varphi = +16°$, $L = 330°$), when a sequence of three proton flares (June 10, 14 and 16), whose geophysical displays were also very important (Symposium, 1959), were observed. We can enumerate some other similar groups with proton flares which had much in common with the considered A. R. (Ogir, 1967a; Severny, 1964a). The comparison of our observations of the flares of 2nd, 4th and 11th August with the observations made at the Big-Bear Observatory (USA)** on 2nd and 7th August showed a great similarity in the development of the phenomena. And, although a more comprehensive analysis is needed to ground the homology of all proton flares in group N 223 (331), nevertheless, one may state that the characteristic features of 4th August flare, considered below, were repeated in all the proton flares of this group and that they are rather typical of many other intense flares.

The 4th August was preceded by the following peculiarities in the development of A. R.:

(a) On basis of totality of the photospheric photographs of the group, obtained at different observatories for the period from 3^d23^h to 4^d06^h, one may see that the umbra of the N-polarity, largest in area, was divided into three umbrae: the main one and two neighbouring ones, which are seen in Fig. 2. Using only the photographs taken at $3^d23^h01^m$, $4^d03^h28^m$, $4^d03^h48^m$ UT one can see that this division of the umbra, which apparently deter-

* It should be considered that the event of four great proton flares in one and the same group within one half-rotation of the Sun is really a rarity.

** The authors are very grateful to Prof. G. Zirin for providing a copy of a film of the chromosphere, taken during the August active period at the Big-Bear Observatory.

mined the changes, having occurred in the structure of the group magnetic field predetermining the flare, took place at $\simeq 4^d02^h$, i. e. $\simeq 3^h$ before the flare commencement. The umbra components were displaced in the south-west direction. This certainly should cause a shift of the intense

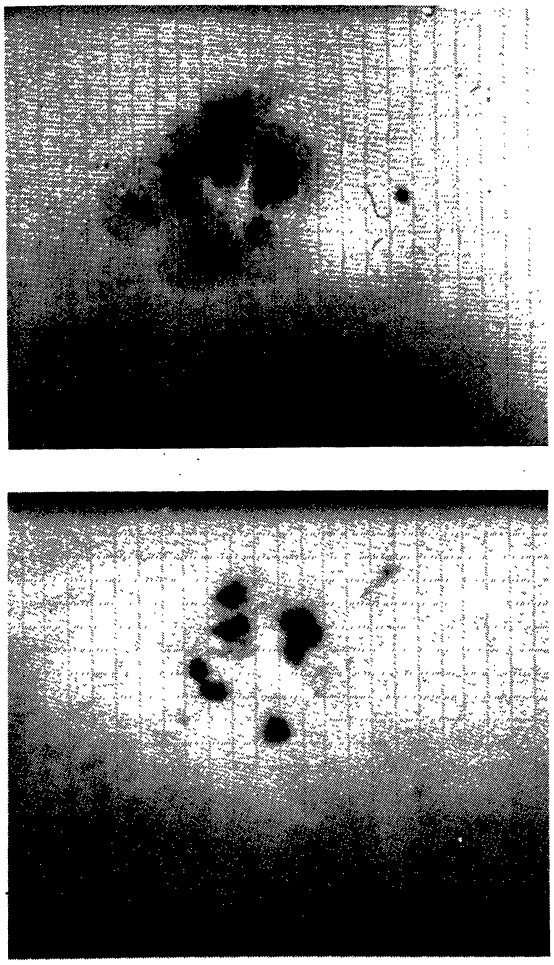

Fig. 2. Variations in umbra of group 223 (331) (a) the photograph was obtained on $3^d23^h01^m$ (Us.S.O.) (b) the photograph was obtained on $4^d8^h05^m$ (Kis.G.O).

magnetic field of N-polarity relative to the "immobile" neighbouring field of S-polarity. However, it should be considered that such motions of the central umbrae of S-polarity, relative to the semicircle of surrounding umbrae of S-polarity, were observed on other days as well. Of particular importance were the motions and variations in the group on 5th, 6th and 8th August when there were no great flares. Note also that, according to the photographs of 2nd, 3rd and 4th August, the dark filaments of the spot penumbra give a good outline of the vortex structure near the divided umbra. At the same place of the field "vortex stresses" a very intensive motion occurred of the chromospheric matter during the flare (Mogilevskii, 1973; Dare et al., 1973). This shows the possibility of existence of a "dynamo effect" in the spot, which could be established more definitely if more comprehensive data were available.

(b) The magnetic field distribution in the spot and its neighbourhood at the time of the flare are represented in Fig. 3 (see p. 84). This magnetic chart of the longitudinal field of A. R. is the combination of the chart obtained at $3^d23^h09^m$ UT with the help of a magnetograph at Kitt-Peak Observatory (USA)* with detailed photographic measurements ($4^d09^h04^m$ — $04^d09^h36^m$) of the field in the spot, made at IZMIRAN.** Such combination was necessary because the magnetograph was measuring the fields $\lesssim 500$ G (in some charts $\lesssim 1200$ G), i. e. it did not fix large fields of the umbrae which could be measured well and in detail on our spectrograms. The magnetic flux in the umbrae of N-polarity exceeded the flux of S-polarity more than three times. This difference (like previously in the papers by Severny 1967, 1970, 1960a,b), reached its greatest value before the flare. Compactness in the location of N-polarity umbrae, predominating in size, and umbra areas determined the peculiar structure of the magnetic field in the chromospheric and coronal fields (Altschuler, Trotter, 1973), as well as the character, spatial distribution and orientation of chromospheric ejections in the flare. It is impossible to estimate the real variations of the field in a flare if no detailed magnetic chart has been obtained before, during and after the flare. It should just be noticed that the comparison of the Kitt-Peak Observatory magnetic charts for $3^d23^h09^m$ and for $4^d14^h08^m$ show the growth and appearance of N-polarity magnetic fields in the southern part of A. R., and the appearance of new fine-structure areas of the N-polarity field in some parts of the S-polarity

* The charts of the longitudinal magnetic field for 2nd, 3rd and 4th August for various lines (Fe 5233 Å, Mg 5173 Å and H_β) obtained with the solar tower telescope of the Kitt-Peak Observatory were kindly sent to us by Dr. W. Livingston. The authors are very grateful to him for them.

** Very prolonged observations of AR were made with the IZMIRAN tower telescope and the IPF-H_α "Opton". Therefore, the solar vector-magnetograph could not be used with the same telescope. To receive detailed data on the field distribution in the spot a frequently repeated survey was carried out (30—50) of polarizational spectrograms in different parts of the spot.

spot (especially near the changed light bridge of the spot). According to Livingston (1973) and our measurements, the gradients of the magnetic field were increasing during the preflare period from 0.4 G/km in some places, which is characteristic of the preflare situation according to (Zvereva et al., 1970; Severny, 1964). The interpretation of the spectrograms of field of spots became complicated due to large field gradients in the spot, the large value of the $H_\perp$ component of the field, and the presence of a number of areas (in the penumbra and at its outer boundary) with an alternating magnetic polarity. This also gives no possibility of distinguishing probable changes of the field in the spot related to the flare in the background of the evolutional changes in the group.

Emission Phase of the Flare

For a more complete study of the nature of the emission and the eruptive phenomena in the flare, let us distinguish its two phases — emission and eruptive. The flare emission in H_α usually determines the commencement, maximum and decrease of a flare. Various eruptive ejections, rise and descent of the chromospheric matter over the spot, characteristic components of radio-bursts related to ejections — these and some other displays of the flare, referred to the eruptive phase, are shifted in time with respect to the flare commencement and become especially intense *after* the maximum of the flare emission. Although the eruptive phenomena in flares have been studied by many authors (Ogir, 1967a, b, 1968; Zvereva and Severny, 1970; Bruzek, 1964; Gopasyuk, 1964; Slonim, 1969, 1970), we think that they were not considered as important as the emission phenomena. This follows, for example, from the character of nearly all elaborated theories of flares which explain the emission phenomena in flares. As will be seen below, the eruptive phenomena in flares cannot be directly connected with the impulsive character of the initial energy emission, and the hydrodynamics of the flare are not a direct result of the emission phenomena. In accordance with one of most elaborated theories (Syrovatsky, 1970) and according to observational data, the emission phenomena in the flare can be divided into the following three stages: initial, explosive and decreasing. The initial "lifeless" stage of the 4th august flare (or, perhaps, preflare) should be considered from 05^h28^m UT, when a typical growth of the emission in the flare was observed by some astrophysical and radioastronomical instruments on space vehicles. In comparison with a very intense emission of the second (explosive) stage of the flare, the initial phase emission seems insignificant and this causes some doubts about the correctness in the determination of the flare commencement moment. If one compares the

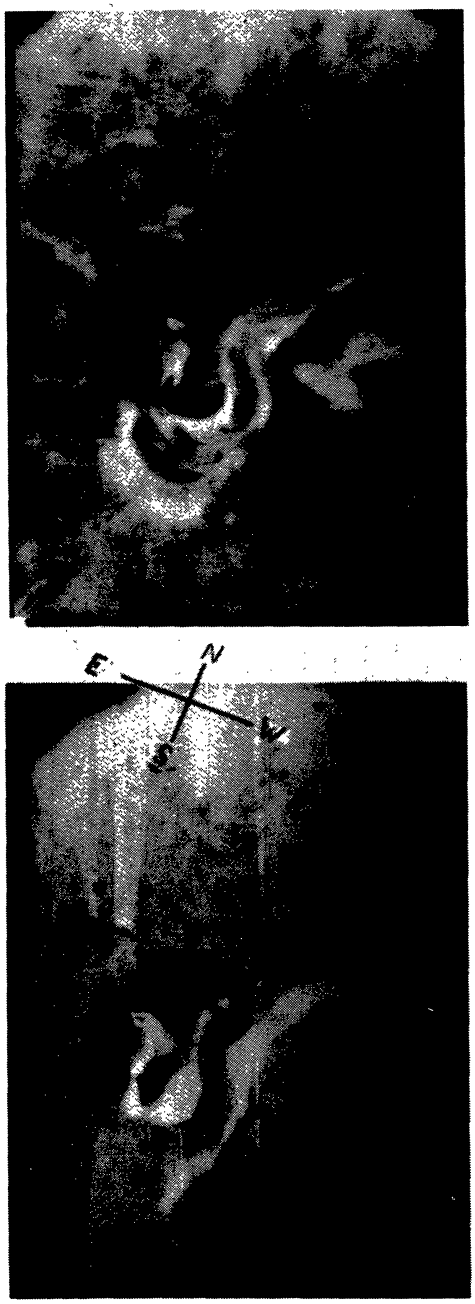

Fig. 4. The initial (a) ($t = 6^h19^m$, $\Delta\lambda = 0.25$ Å, $\lambda_0 = H_\alpha + 0.4$ Å), and (b) the beginning of the explosive stage ($t = 6^h26^m$, $\lambda_0 = H_\alpha + 0.8$ Å) of the flare emission phase.

filtergrams which we took in the period $5^h55^m \div 6^h19^m$ (before the explosive stage) and at 6^h23^m (Fig. 4), a detailed correspondence is seen in the position of the points and thin threads of the emission of the initial and intense emission of the explosive stages. This is the indication of their closest genetic relation. As is seen from this figure, during the initial stage some bright emission points ($d \lesssim 2$—$3''$) are distinguished in the largest umbrae of the spot, as well as some extended thin ribbons near the S-boundary of the filament, "streamlining" the umbra boundaries (Fig. 3), and a light bridge between the umbrae N 1 and N 2 of N-polarity. This light bridge was variable, but it was "burning" continuously during the whole period of the flare. A prolonged existence during the initial stage of the "schematic basis" of the H_α-emission distribution which remained both at a great increase during the explosive stage, and at the flare decreasing, is to be considered as a typical feature of the flare emission distribution.

According to the observations made with the SibIZMIRAN (Irkutsk) radiopolarimeter* an impulsive "B" type outburst with high intensity of emission, remaining in the cm range, was associated with the flare commencement. The same was observed at some other observatories (Report UAG-21, 1972). In the meter-decameter range a continuum and groups of intense type III bursts were seen, although some similar phenomena were observed before the flare as well (Report UAG-21, 1972). The explosive stage of the emission phase began at 6^h21^m with a sudden sharp increase (during $\simeq 2$ min) of brightness and in the size of "stationary" points of emission. In the two S-shaped parallel bright ribbons a fine structure is distinguished which is visible on filtergrams taken at the point $H_\alpha \mp 0.8$ Å (Fig. 5): several points (2—3″) of the emission in umbrae 1, 2, 3 of N-polarity; a thin forked connecting bridge; "flow" of the emission bands round the umbrae, etc. The following features of the two ribbons should also be noted:

(1) Up to the moment of the H_α maximum ($\simeq 06^h38^m$) each of them occupied the region where there were correspondingly only either N or S magnetic field. This "non-contactability" was also observed in the places where the emission boundaries approached close enough.

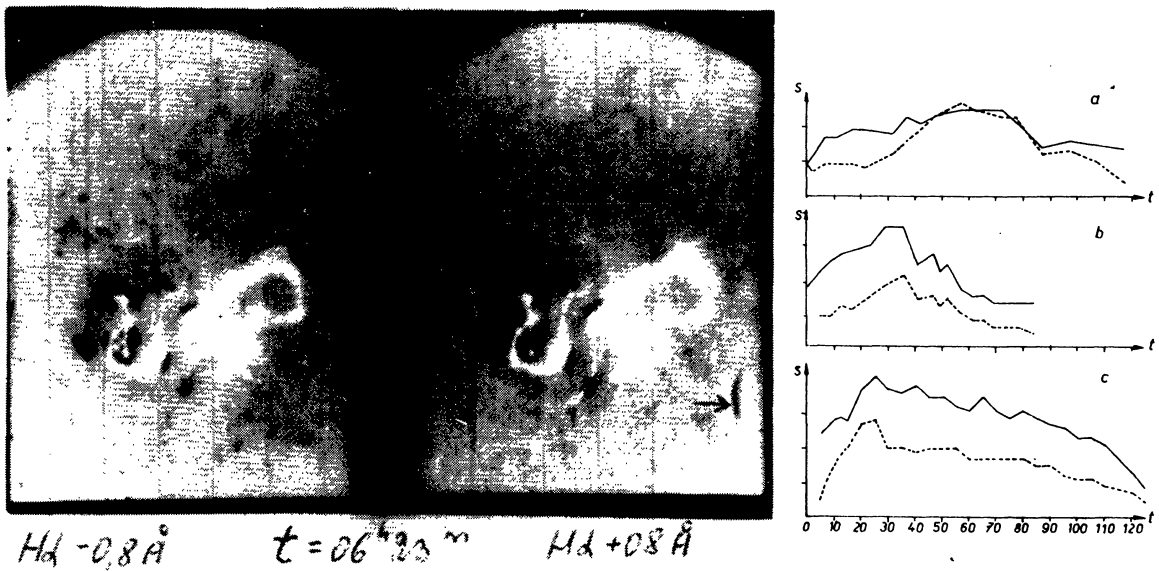

Fig. 5. Filtergram $H_\alpha + 0.8$ Å, $t = 6^h23^m$. Arrows mark the places of filaments in which typical wave motions were observed.

Fig. 6. Changes of the area of two ribbons during the flare: (a) for the proton flare of 2.08, (b) the same for 4.08; (c) the same for the flare of 7.08. The area is given in arbitrary units, the time — in minutes from the beginning of the flare explosive phase.

* The authors thank Dr. B. P. Nefedeva (SibIZMIRAN) for the copies of the radioemission records on $\lambda = 3.2$ cm.

(2) As can be seen from Fig. 6 the changes in the area of each emission ribbon were nearly parallel, even including the individual time variations. Moreover, the area of the ribbon located in the S-polarity magnetic field, was nearly twice as large. It is typical that the same relation of the time variation of the bright ribbon area was also observed in the same group with the proton flares of August 2nd and 7th. The relation between the bright-ribbon areas was the opposite to that of the values of the magnetic fluxes of N and S-polarity umbrae. The brightness in the ribbon of N-polarity (particularly above the corresponding umbrae) was somewhat greater than the brightness in the ribbon of S-polarity.

(3) From a detailed analysis of the filtergrams (particularly of those taken at the contour wings) one can see that at a number of places the bright ribbons consist of spirally twisted thin emission lines (Fig. 7). The twisted emission lines of a cross-section of 2—3″ can be seen especially well above the large umbrae of N-polarity (N 2, 3).

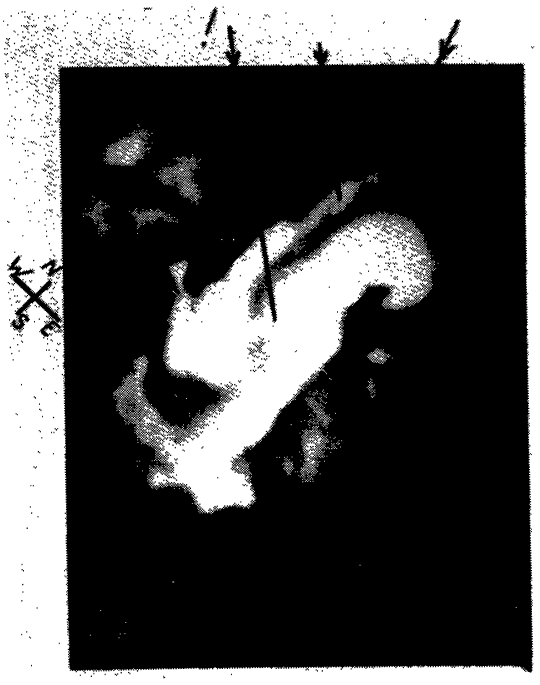

Fig. 7. H_α-filtergram $t = 6^h42^m$, $\lambda_0 = H_\alpha + 0.4$ Å. In marked places a spiral structure of the two-ribbons details and the conjunction bridge between them are seen.

The above-listed features of the two ribbons show that in their formation an essential role belongs to the structure of the chromosphere and coronal magnetic fields with which the source of their emission excitation is associated. Although a growth of the emission ribbons and of brightness oscillation was observed prior to the H_α-maximum in some parts of the two ribbons, both the ribbons still remained rather stable. The dimensions of the S-shaped "path" between them did not change before the appearance of the arch absorption systems. Only after the maximum of H_α could a certain increase of the distance between the two ribbons be seen.

One of the most visible motions of chromospheric matter during the explosive stage of the flare was a considerable quasi-periodic disturbance of the "quiet filament" which then grew into more regular oscillations. This phenomenon will be discussed below, because it characterizes another (eruptive) phase of the flare. The quasi-stationary prolonged absorption ejections of the AFS (Arch Filament System) type into the E-part of A. R. near a single small spot of S-polarity also belong to the eruptive phenomena of the explosive stage of the emission phase (see

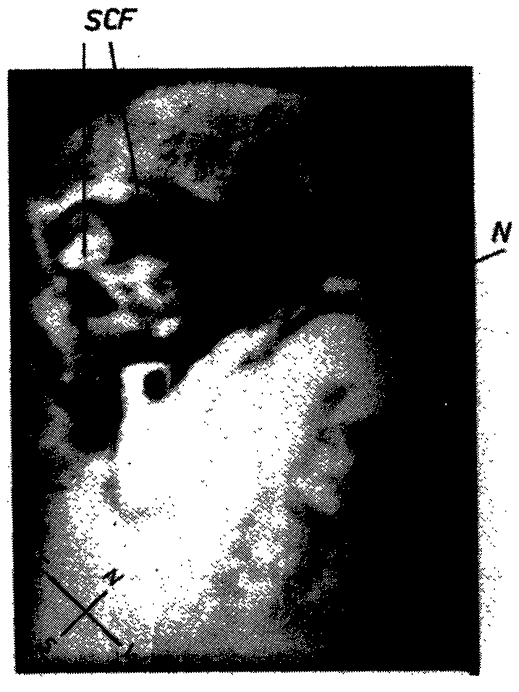

Fig. 8. H_α-filtergram $t = 6^h36^m$. $\lambda_0 = H_\alpha + 0.4$ Å. The sub-flare and an oscillatory structure of the filament are seen.

Fig. 8). From about $\simeq 06^h33^m$ UT a subflare induced by the main flare was observed in the region of this spot. The existence of this relation can be seen well from the filtergrams taken in the centre

of H_α. At the time the subflare commenced the thin absorption arc, connecting N-umbra (N 4, Fig. 3b) and the penumbra of the spot with the area around the single spot S4, was replaced by a thin arc-shaped emission ribbon. It reached the intensity maximum at the same moment that the subflare maximum occurred ($\simeq 06^h47^m$ UT) and went out at $\simeq 7^h03^m$ UT when the subflare went extinct. The subflare looked like flocculae, gradually increasing in brightness, around a small spot surrounded by a complex AFS system. If one considers that the disturbing agent, causing this subflare, began to propagate from the main spot at the time of the beginning of the explosive stage, the everage velocity of its propagation along the connecting arc can be estimated at $\simeq 15$—20 km/sec which is close to the local Alfvén velocity at lower chromospheric altitudes in the region of A. R.

We have no detailed records for the X-ray emission of the flare of 4th August and, therefore, we only note that as follows from Dere et al. (1972) and Report UAG-21 (1972), together with a very powerful flux of hard and thermal X-ray radiation (Chapp et al., 1973) some discrete lines of γ-radiation were first observed at CA OSO-7 during the period of the proton flares of 4th and 7th August. The radiation was observed in the line with an energy of 0.5 MeV which corresponds to the positron-electron annihilation reaction, and in the line of exitated deuterium nucleus (2.2 MeV and others). Under the conditions of the OSO-7 flight, this prolonged radiation of 4th August could only be recorded till 06^h33^m UT (before the maximum of H_α), while, on the contrary, during the flare of 7th August the orbital position of the vehicle allowed this radiation to be observed only after the maximum of H_α (from 15^h26^m UT to 16^h09^m UT). The existence of the emission in the γ-lines is usually associated with nuclear reactions which could occur in the presence of powerful fluxes of overthermal particles in the solar atmosphere. The long existence of such fluxes of high-energy particles during the whole period of the proton flare, as well as the prolonged polarization of hard X-radiation observed from CA "Intercosmos-7" (Tindo et al., 1973) was possible only under the condition that the energy production and the generation of electron fluxes, directed along the magnetic field, occurred and continued in the flare for a long period of time. This important condition should be taken into consideration in discussing the comparable role of the emission and eruptive phases in the flare.

An intense and prolonged multicomponent type IV radio burst is associated (Akinyan et al., 1972) with the beginning of the explosive stage in the emission phase. Its microwave component IVμ appeared at 06^h18^m UT and continued for $\simeq 240$ min. Near the maximum ($\simeq 06^h35^m$ UT) its intensity on 8800 MHz was $\simeq 3.6 \times 10^{-18}$ wt m^{-2} Hz^{-1}. During the burst maximum an inversion of the circular polarization sign was observed on 3000 MHz.

Eruptive Phase of the Flare

Let us consider in greater detail the important phenomena of the eruptive phase of the flare.

(a) *The motion of chromospheric emission matter.* In a number of papers of the Crimean Observatory, as well as in the papers of some other authors (Ogir, 1967a,b, 1968; Severny, 1964a,b; Zvereva, Severny, 1970; Bruzek, 1964; Gopasyuk, 1964; Slonim, 1969, 1970) the motion of bright emission bands of the flare was analysed. During observations of these phenomena on the disk (in contrast to limb phenomena) it is rather difficult to distinguish real motions of luminous chromospheric matter on the background of variations connected with the change of emission conditions. Frequently observed changes of the two ribbon boundaries (increase of the distance between them) most probably reflect the replacements of the energy source (Sturrock, 1967). During the flare of 4th August these divergences of the band of two ribbons were insignificant. The emission regions on the filtergrams, taken at symmetrical points of the contour, were the same on the average, although in some places (over great umbrae of N-polarity, over the great umbra S2, near the quiet filament) a visible difference was observed. In fine-structure emission details this asymmetry becomes particularly visible.

Near the epoch of the flare maximum, between the inner boundaries of the two ribbons, a large emissional "tongue" appeared which then connected the inner boundaries of the two ribbons. The axis of this connecting bridge was directed towards the line of band separation ($H_\parallel = 0$) under a large angle ($\simeq 25°$). The first front of the emission "tongue" protruded from umbra N2 in the NE-direction towards umbra S2. The average velocity of its distribution was 2—$3 \cdot 10^7$ cm/s.

Along the inner boundaries of the two ribbons and along the connecting light bridge some thin absorption filaments were observed. The development of these filaments and the appearance of arch flare ejections (AFFS)* afterwards fully "absorbed" the emission bridge. In the given case, as can be seen from the Dopplerograms (Fig. 9), we had a real displacement associated with a rising spiral motion of the chromospheric emission matter between the two ribbons. Simultaneously with the increase of the velocity from 4 to 10 km/s, the motion along the magnetic lines of force was observed (it can be seen well in the AFFS) with a velocity $\gtrsim 10^7$ cm/s. The latter phenomena is also confirmed by the spectrograms in (Sitnik et al., 1973). The appearance of the temporary connecting emission bridge between the two ribbons determines the phenomena of the "Y-phase" (Křivský, 1963; 1965; 1966) to which the process of solar cosmic-ray (SCR) generation is attributed.

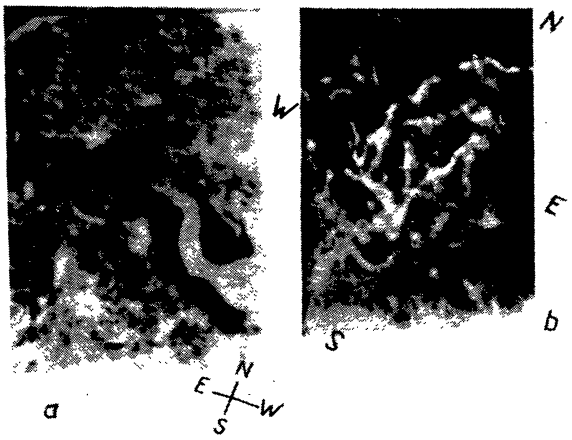

Fig. 9. (a) Dopplerogram near the flare maximum. Light places — V_D — from the observer, dark ones — V_D — towards the observer. The places of two ribbons were not subtracted due to overexposure. Oscillatory movements in the filament are visible.

In the given case it is important that the "Y-phase", well-defined in details by our high-resolution filtergrams, came 15—17 min *after* the commencement of the explosive flare stage. This means that in respect of energy the "Y-phase" is hardly connected directly with the initial impulsive ($\Delta t \lesssim 2^m$) energy production at the beginning of the explosive stage in the flare emission phase.

* Since the systems of arch flare ejections considerably differ by their parameters from similar phenomena with no flare, we shall designate them conditionally as "Arch Filament Flare Systems" (AFFS).

(b) *Motions of the "quiet" filament.* The filament, which will be discussed below, was located along the neutral line off $H=0$ (Fig. 3b) in the northern and north-western parts of the A. R. It was fully formed on about 1st August. In spite of a series of intense proton flares and a great deal (>50) of weak flares, the filament was observed without noticeable changes on all days, including 11—12th August, when the group went beyond the W-limb of the disk. To the east of the A. R. this filament continued in the form of another large filament which stretched in the latitudinal direction $\gtrsim 90°$. From time to time some breaks with subsequent conjunctions were observed in this other filament, and by August 9—10th a decay occurred in the series of AFS. These changes, as well as the quasi-periodic disturbance in the A. R. filament, were associated with intense flares. The disturbances in the "quiet" filament during the 4th August flare were of a complex character. Their detailed study on the basis of our filtergrams is an independent problem. We shall describe in general only the quasi-periodic variations which are necessary for discussing further the energetics of the flare eruptive phenomena. Starting from $\simeq 06^h24^m$ UT an intense rise was observed of the matter of the peak (northern) of the filament curve and a sharp fall on the other two sides of this formation. The extent of the rising part was $1.3 \cdot 10^9$ cm, and of the falling ones $\simeq 10^9$ cm. Maximum velocities were $\simeq 45$ km/s. The quasi-period of these disturbances was ~ 420 s, and thy were repeated 2—3 times during the decrease. At the same place an emissional "background" was observed, the intensity of which also changed in accordance with the filament disturbances. Southwards along the filament, from 06^h28^m UT, a disturbance was observed which was like a twist of the filament ribbon with the extent of $2 \times 35''$. The amplitude of the latitudinal deviations reached $\lesssim 10''$. In the next part of the filament (extent $\sim 20''$) over an interval of 400 s after flare commencement and from 06^h37^m UT to 07^h17^m UT, the matter was observed to rise with a velocity of 25—30 km/s. During the post-maximum period of the flare in some places along the filament some quasi-periodic ($t \simeq 15$—20^m) latitudinal deviations were observed with amplitudes $\lesssim 5''$. Thus, before the flare maximum in the "quiet" filament some strong longitudinal (in radius) quasi-periodic ($t \simeq 4.2 \cdot 10^2$ s) fading disturbances were observed. Simultaneously with the longitudinal (in radius) disturbances, latitudinal

impulsive quasi-periodic deviations were also observed, which had rather large amplitudes until 06^h45^m UT and rather small deviations during the next period of the flare. An example of the large disturbances in the filament is shown in Fig. 5.

Note that, according to Akinyan et al. (1973), the source of the quasi-stationary component of the IVmB burst was directly associated with a closed magnetic configuration of the field over this filament. A peculiarity of the radio emission of this component, with its exceptionally great intensity ($\gtrsim 10^{-18}$ wt $m^{-2}Hz^{-1}$) in the frequency band III-23 MHz (maximum $f = 40$ MHz), was a quasi-periodic very deep modulation of the intensity and polarization observed for quite a long period of time. This phenomenon of deep modulation, associated with the oscillations of the magnetic field in the IVmB source, was induced by impulsive and quasi-periodic disturbances which were observed in the "quiet" filament.

(c) *Arch Filament Flare Systems (AFFS)* are observed in all proton flares as noted by many authors (Bruzek, 1970; Roy, 1972; Zirin, Tanaka, 1973; Koval, 1972). They are the most typical phenomena of the eruptive flare phase. According to AFFS investigations (Slonim, 1970; Roy, 1972), spectral and dynamic characteristics which were observed either on the disk or at the limb, as well as their connection with radio and X-ray emissions, all indicate that this really powerful eruptive phenomenon in the flare embrases both the chromosphere and the A. R. corona and is a real flare-born phenomenon.* In our case various AFFS were observed and were connected mainly with a general rise of chromospheric matter in the dark space between the two ribbons. Although the first AFFS appeared before the maximum of the H_α-emission, the principal AFFS were seen on the curve of the emission-phase decrease. The general concept of the main AFFS of the 4th August flare is represented in Table 1 and in Figs 10, 11, 12. (Fig. 10 see p. 84). On the basis of the analysis of our filtergrams the following conclusions can be drawn:

(1) All observed AFFS "leaned" with their opposite ends in places with N- and S-polarities, i. e. the system of fine-structure arches were oriented along the lines of force and crossed the neutral line ($H_\parallel = 0$) preferentially under an acute angle (if there is a shift in height under a definite angle). This conclusion follows from the superposition of filtergrams with AFFS over the chart of either the photosphere or chromosphere (in the H_β line). Figure 11 shows an example of such locations of AFFS. This agrees with the results obtained by some other authors (Roy, 1972; Zirin, Tanaka, 1973).

Fig. 11. H_α — filtergram $t = 8^h02^m$. $\lambda_0 = 0.0$. Some AFFS arches are marked with arrows.

(2) Systems of thin fibres ($d \lesssim 2$—$3''$) consisting of several (from 2 to 10) absorption filaments at first rose with a velocity of 15—25 km/s. At the end of each phenomenon the velocity decreased to 8 km/s.

(3) The velocity of motion of the head of the filament, which could be measured on filtergrams taken at different points of the contour, reached 150—200 km/s. This can be seen well in Fig. 12 where the filaments are visible in the far distant blue wing and disappear in the red wing. Similar velocities for some AFFS were obtained from the spectrograms of the 4th August flare in the paper by Sitnik et al. (1973). The above-mentioned characteristic parameters agree well with the results of previous papers (Roy, 1972; Zirin,

* In references to flares AFFS the term: "post-flare loops" occurs (Zirin, Tanaka, 1973) because they are observed after the maximum of the H_α-emission. Many authors, however, consider the flare-born phenomena to be phenomena of the flare itself (Bruzek, Demastus, 1970; Roy, 1972; Frazier, 1972).

Table 1

NN	Time of commencement	Duration in min	Number of arches	Average length of arches	The character of the system development
1	06^h26^m UT	12	10	55″	Weak arches distributed all over the 55 × 33″ area. Formed at the place of a weak emission, which was present at the initial stage of the flare.
2	06 23	100	4—5	45	Long-existing system in the southern part of the A. R. Suffered considerable changes. At 06^h47^m in this system two arches appeared which reached the size of ~ 77″ after twisting and elongation. By 07^h04^m UT a new system had been formed as a toroidal surface.
3	06 51	90	10	35	Distinguished from system (2). Was located across the emission ribbon of S-polarity and at an angle of 35° to system (2). From 07^h18^m — 07^h29^m arches appeared in the southern part with $l \simeq 25$—30″ at an angle of ≃ 10° to the northern part of (2).
4	06 47	20	5	30	System above the "quiet" filament near the spot.
5	06 48	10	2	25	System in the northern part of the ribbon of S-polarity.
6	07 17	70	10	20	Appeared in the region of system (4) forming with it an angle of ≃ 30°. Maximum was reached at 07^h24^m.
7	07 19	12	5	35	System of arches across the filament in the region of systems (4) and (6). Great rates of ascent ($V_z \simeq 50$ km/s) were seen at the period of maximum development 07^h25^m – 07^h26^m.
8	08 11	10	6	25—40	Were formed in the region of system (6). One arch approached umbra S2.
9	07 05	25	4	20	Arches were sharply turned at the ends towards the photosphere.
10	07 18	70	10	10	Were located more to the south and at an acute angle to system (2).
11	08 02	20	6	45	In the greatest arch with thickness ~ 6″ the rate of ascent was 50 km/s. At 08^h05^m — forked the initial part of the arch.

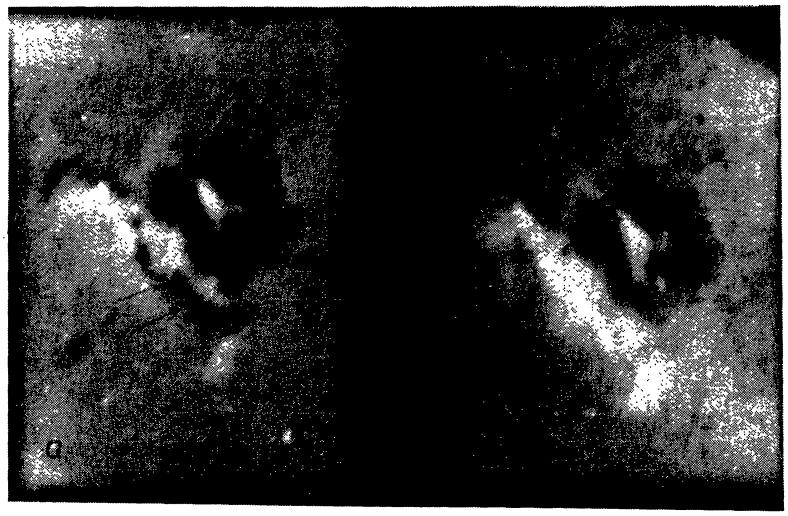

Fig. 12. H_α — filtergrams $t = 7^h30^m$. (a) $\Delta\lambda = 0.25$ Å, $\lambda_0 = H_\alpha$ — 1.2 Å. In the far wing some AFFS are visible, while at (b) ($\Delta\lambda = 0.25$ Å, $\lambda_0 = H_\alpha + 0.6$ Å) AFFS are not observed.

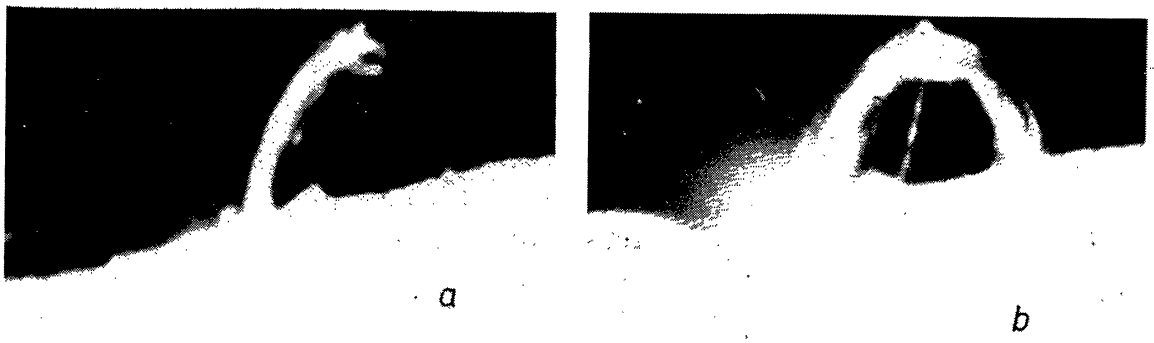

Fig. 13. Examples of LPS ≡ AFFS during the limb flare of 11.08.72

Tanaka, 1973; Koval, 1972). Note also that, contrary to the great dispersion of velocities during flare-born phenomena of the "mustaches" type (Koval, 1972), in AFFS the velocity of matter along magnetic lines of force is nearly homogeneous (spread $\simeq 15$—20 km/s) (Sitnik et al., 1973).

(4) During the proton flare of 11th August which occurred when A. R. went beyond the W-side of the limb, we filmed AFFS-phenomena (the system of arch prominences — "Loop Prominence System" — LPS). Figure 13 shows that a very thin ($\simeq 2$—3″) thread-shaped system of ejections was directed along the magnetic lines of force. This follows from the comparison of the filtergrams with the lines of force of the A. R. magnetic field above the group, calculated in (Altschuler, Trotter, 1973). The height to which the arches rose reached 5—7 . 10^9 cm. It is characteristic that sometimes the emission arches condensed and increased in brightness and then a widening loop prominence was established (Fig. 13). Note also that both in AFFS on the disk and in LPS the movement occurred mainly from the region of N- to S-magnetic polarity. The LPS fan condensed near the regions of N-polarity and greatly widened where the S-polarity decreased. This characterizes (see below) the peculiarities of the magnetic field in the chromosphere and corona over the spot.

(5) As is seen from Table 1, in some places (systems N 2, 3; 2, 11; 4,6) the AFFS, located at different altitudes, were crossed. It is also characteristic that the AFFS over the initial part of the "quiet" filament, near spot S2, was at a considerable angle to the filament. At 07^h02^m UT in the southern part of the spot, the AFFS, being located at various altitudes, crossed at right angles.

Other Types of Eruptive Phenomena. Let us note briefly also the following eruptive phenomena, occurring during the flare:

(1) A long-lived system of arch filaments (AFS) in the region of a single small spot 4 of S-polarity where a subflare was observed (Figs 4, 8).

(2) The ejection stemming from a large spot of S-polarity (S3, Fig. 8) existed for more than an hour. This long ($l \simeq 65'' = 5 \cdot 10^9$ cm) ejection of variable intensity consisted of thin thread-shaped filaments, along which the velocity of the matter was $\simeq 70$—80 km/s. At the points where these filaments decreased, there was a floccula located at an N-polarity magnetic "hump", i. e. in this case the motion went along the lines of force.

(3) From 7^h05^m UT an very long ejection occurred in the southern direction from the region of the same S-umbra (S3, Fig. 8), i. e. perpendicularly to the ejection sub (2) towards a small isolated hump of N-magnetic polarity. Ejections (2) and (3) then grew into stationary AFS.

We shall not enumerate any more eruptive phenomena of lesser interest, but only mention that common for them all (both strong and weak ones) was the motion of matter *along* the lines of force of the magnetic field which connected umbrae or magnetic humps of *opposite* polarities, and this motion occurred, as a rule, in the direction from N- to S-polarity. Unlike these fine-structure absorption ejections, the emission bands connected the umbrae of the *same* magnetic polarity. Absorption ejections lived for a long time and were observed out of any connection with the commencement of the explosive flare stage. It is also of importance that the comparison of optical and radioastronomical observations (Akinyan et al., 1973) showed a close genetic relation of the AFFS with the source of the decimeter component of radio IV dm bursts which certainly has a profound physical meaning.

Discussion

Let us perform a rough estimate of the energy which is necessary to generate some principal eruptive phenomena in a flare.

We shall first determine from the parameters measured on filtergrams the energy in one elementary filament of the AFFS. The absorption arch of the AFFS, as described above, represents a plasma tube ($l \simeq 2 \,.\, 10^9$ cm, cross-section $S \simeq 10^{17}$ cm^2) frozen into the magnetic field. It rose from the initial height of $h_1 \simeq 2$—$3 \,.\, 10^8$ cm to $h_2 \simeq 8 \,.\, 10^9$ cm at an average velocity of $V \simeq 1$—$2 \,.\, 10^6$ cm/s. Absorption filaments are clearly visible on bright flare emission ribbons, whose intensity, according to the measurements of Hyder (1966), became three times higher, at the moment the AFFS appeared, than in the non-disturbed chromosphere. With regard to the geometrical parameters of the arch filaments given, this means that the optical thickness $\tau \gtrsim 1$ is achieved, if the hydrogen concentration in it is of the order of 10^{13} cm^{-3}.* Then, the energy which is necessary to form one arch will be $\varepsilon \simeq 2.4 \,.\, 10^{29}$ erg. The kinetic energy of the movement of chromospheric matter, $M \simeq 1.2 \,.\, 10^{15}$ g, with a velocity of $V \simeq 2 \,.\, 10^7$ cm/s along the filament, will be of the same order. Since the motion (rise) of the filament takes place against the magnetic forces until it reaches the maximum of its ascent $\beta = \frac{8\pi P}{H^2} \gtrsim 1$, the change of the magnetic field energy must be either not less than or of the same order as the value we obtained ($\varepsilon = 2.4 \,.\, 10^{29}$ erg).

According to the data given in the Table 1, in different periods of time, no less than 11 different AFFS were observed during the flare. From 2 to 10 (and even more) filaments existed in each of these AFFS. Hence, we find that the lower boundary of the overall value of the energy, related to the AFFS, is of the order of 10^{31} erg. Note for comparison, that in accordance with the measurements of Zirin and Tanaka (1973) the emission energy in H_α for the 4th August flare is $2 \,.\, 10^{30}$ erg.

Note, that a similar estimate of the energy of other long-existing absorption ejections gives values comparable (and even exceeding) with the energy of the H_α-emission. The energy needed to swing the "quiet" filament may be estimated by applying calculations of filament and prominence oscillations in magnetic field, performed by Hyder (1966). In our case, only for the initial swing in the upper part of the filament (where vertical oscillations with periods of 420 s were observed, whose fluctuations continued three incomplete periods) it is necessary to have an energy of $\simeq 8.2 \,.\, 10^{27}$ erg. The effect of magnetic fading-out may be used to estimate the magnetic field in filaments $\simeq 70$ G. Since the disturbances in the filament (as is seen from observations) looked like successive fluctuations (not less than four) of individual, more prolonged quasi-periodic disturbances, the total energy of the filament distribution should not be less than $7 \,.\, 10^{28}$ erg. Although this value is much less than the overall energy of the AFFS, it is sufficient (Akinyan et al., 1973) to excite radio emission oscillations in the IV mB source of the component.

The estimates mentioned above show that even if all the losses are not considered by far, the energy of the eruptive phenomena in the flare is not only comparable, but apparently exceeds the energy of the emission phenomena. The principal difference between them is in that for the emission phenomena the energy source is local and occur preferably as an impulse ($\Delta t \lesssim 2^m$) during the explosive stage, while, according to observations, the sources of the eruptive phenomena exist for a long time (practically during the whole period of the flare) and are scattered all over the A. R.

In order to understand the various natures of these sources, let us discuss one of the possible phenomenological patterns within the flares, by which it is possible to explain qualitatively the eruptive phase of the flare. Consider the magnetic field structure at locations where the AFFS exists.

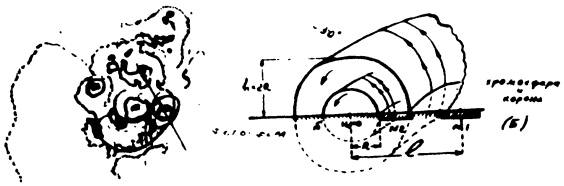

Fig. 14. The pattern of the toroidal field model in the region of AFFS.

The whole arch "dome" of the AFFS, enveloping the whole curved region between the two ribbons with the neutral line ($H_\parallel = 0$) as the axis, may be schematically considered so as it is shown in Fig. 14, as a part of a toroid. In this case, the centre of

* $\tau_2 = K_2 N_2$, where N_2 is the number of H-atoms in the second quantum state along the line of sight (d). Turning to the number of atoms in the main state (if $T \simeq 6.10^3$ K) $N_0 \simeq 10^5 N_2$ we obtain (if $K_2 = 3.10^{-13}$) $N_0 \geq 10^{13}$ cm^{-3}.

the large circle of this toroid will be the large umbra of N-polarity (N1) which represents the real centre of the relative displacement of the S-field of spot, relative to the N-field (Morozov, Solovev, 1963). The radius of this large circle is $\simeq 55''$ ($4 \cdot 10^9$ cm), while the radius of the small circle of the toroid, whose lower part passes under the photosphere, is about $15''$ ($1.1 \cdot 10^9$ cm). As can be seen from observations (Table 1, Fig. 10), an outer toroidal magnetic surface must be located around the toroidal magnetic surface, the smaller radius of which is twice as large as the inner one. It is typical that the AFFS at the outer toroidal surface are at a significant angle ($\gtrsim 35°$) to the AFFS at the toroid. This "shear" of lines of force, shown above, may define the stability of the considered closed magneto-plasma configuration. For our estimate we may use the data of the equilibrium magneto-plasmic toroidal systems, computed in detail in Solovev, Shafranov (1967); Morozov, Solovev (1963). For the spiral field of our model the scalar potential in cylindrical co-ordinates will be

$$\varphi_B = z - A\varphi + BK_1(z) \sin \vartheta \,, \qquad (1)$$

where A, B are constants computed for a given model and $K_1(r)$ is the modified Bessel function. We accepted in (1) the model of a spiral field with a "winding" on the inner cylinder (Solovev and Shafranov, 1967) because this corresponds qualitatively to our observations. Using the graphical computer results for the magnetic field of this model, given in Solovev and Shafranov (1967), we were able to determine the required parameters of the field and compare them with our observations. In our case the measured magnitude of the relative "shear" for simultaneously existing AFFS, both at the inner and outer toroid, was equal to 0.61. Then, according to Solovev and Shafranov (1967) the longitudinal magnetic flux (reduced to a relative value at the photospheric level) will be 0.04. The specific volume of the magnetic field

$$V'(\Phi) = \int \frac{\mathrm{d}l}{B} = \frac{L}{\langle B \rangle} \,, \qquad (2)$$

for $V = 3.2$ will be equal to 2.6 (with our value of L). This allows one to obtain the values of the constants A ($= -2.8$) and B ($= -1.4$) for the scalar potential φ_B. The knowledge of the latter solves the problem of determining the magnetic field in the adopted model.

Now, compare the adopted model with the observations. Up to the height of $h = 2.2 \cdot 10^9$ cm (according to our model) the plasma with the field in the toroidal dome is stable. Due to the relative shear of the lines of force at the outer and inner surface of the toroid, a convective stability is established. This can explain the fact that in the presence of a disturbance some inner arches of the AFFS were sometimes increasing impulsively from $\simeq 25''$ up to $50''$, but within several minutes they were again back to their initial size $\simeq 25''$. In the model of the field under consideration, there exist conditions for a comparatively long existence of magnetically trapped overthermal particles (Solovev and Shafranov, 1967). The existence of traps for high-energy electrons is confirmed by the close connection of the AFFS phenomena with the radio-emission source of the IV dm component (Akinyan et al., 1973). The generation of these overthermal electrons may be connected both with the initial impulsive acceleration due to the passage of a shock wave, or (which is also possible) with the mechanism of a long-period statistical acceleration in the inhomogeneous magnetic plasma with changes and appearance of the AFFS. In spite of considerable changes in the AFFS, seen in Table 1, the characteristic sizes of "two doms" were preserved during the whole period of our observations. The AFFS measurements during the 7th August flare give nearly the same characteristic AFFS parameters as for the flare of 4th August. The measurements at the LPS ≡ AFFS limb show the presence of two systems of lines of force sheared relative to each other. At the same time, the limb observation data of an intense eruptive ejection above the AFFS (Bernes and Kusoffsky, 1973) show that at heights over $L = 2R = 2.2 \cdot 10^9$ cm the configuration of the magnetic field is open. The magnetic field above the "quiet" filament, near the initial part of which (near the spot) a stationary AFFS was observed, should have a closed configuration. This agrees with the configuration of the coronal field calculated in Altschuler and Trotter (1973), in which both: the closed configuration above the filament and the closed configuration but with a transition into an open one (above the spot where nearly all AFFS were observed), are distinguished.

How should one imagine, in our case, the formation of a "shear" and the transition of the closed field system into an open one? The main energy source for the non-equilibrium phenomena in the A. R. are the time variations of the group

magnetic moment, connected with the variations of the magnetic field in the course of a relative motion of umbrae of opposite polarities. The existence of such relative shear follows from the measurement of the group umbra co-ordinates (Pfister, 1973).* The relative shear of the fields of opposite polarities was observed in the spot on all observational days. Nearly 3 hours before the flare of 4th August the value of the relative velocity of the umbra displacement (at the division of umbra N2) was estimated at about $4 \cdot 10^5$ cm s^{-1}. Using the chart of the magnetic field, one can calculate the rate of change at the given magnetic momentum: $\left|\frac{\Delta \vec{M}}{\Delta t}\right| \simeq \left|\Phi \frac{\Delta l}{\Delta t}\right| \simeq 7.5 \cdot 10^{26}$ Mx s^{-1}. In the volume between the toroidal surfaces (Fig. 14) ($V \simeq 10^{28}$ cm^3) at an average plasma concentration $\simeq 10^{11}$ cm^{-3}, an energy of about $3 \cdot 10^{31}$ erg must be produced, which corresponds to the energy of eruptive flare phenomena. The peculiarity of the umbra motions, observed at that time was the displacement of the central umbrae of N-polarity relative to the surrounding umbrae of S-polarity. In Rust (1973) it is also stated that from the measurements of photospheric magnetic charts a reversal of the S-polarity magnetic fields was observed relative to the "immobile" central N-polarity fields of the spot. The analysis of the magnetic charts and filtergrams show that this reversal took place around the axis crossing the umbra N 1, which was accepted in our model as the centre of the toroidal magnetic surfaces. As a result of the relative displacement of the magnetic fields (cf. Sturrock, 1972; Roy, 1972): (a) a "shear" of the magnetic lines of force on the closed toroidal surfaces must occur; (b) at heights of $h > 2R_1 = 2.2 \cdot 10^9$ cm (in our model of the field) the process of reconnection of lines of force must occur with a formation of an open field configuration. The process of relative displacement of the magnetic fields was observed with one intensity or another during the whole observational period, which could stimulate the long existence of an open field configuration in the corona above the group. The region of formation of an open current surface (Sturrock, 1967, 1972) is where the flare energy is generated.

* Analogous measurements were performed by Z. B. Korobova for a number of filtergrams. In her measurements the absolute co-ordinates of all umbrae are given, while in Pfister (1973) the co-ordinates of shear, relative to the large umbra, were determined.

At present it would be premature to discuss the mechanism of AFFS formation and development, because we lack sufficiently complete qualitative characteristics of both the individual elements and the whole complex of the considered eruptive phenomena. One cannot define, for example, whether the magnetoplasma tubes of the AFFS are "frozen" into the general force-free magnetic field (see, for example, Solovev, 1971), or whether they consist of discrete magneto-plasma elements (Mogilevskii, 1970); what is the nature of the filament oscillations; what is the mechanism of the chromospheric plasma ejection, etc. In order to illustrate the time pattern of some of the basic phenomena in the flare of 4th August, Fig. 15 is presented. The direct, although not fixed, generation of low-energy solar cosmic rays, whose energetic spectrum differs from the SCR of initial generation (Dorman and Miroshnichenko, 1968), as well as the generation and escape from the A. R. geoeffective corpuscular fluxes, are referred to the eruptive stage of the flare due to the following:

(1) Sufficiently comprehensive observations of great solar flares (importance $\simeq 2$), which took place in the A. R. without spots (or with very small spots) (Dodson and Hedeman, 1970) indicated that inspite of a large area and brightness of the flare-born floccula, the long-existing emission phase of these flares was not accompanied by eruptive phenomena. Such flares, at any location relative to the central meridian, are always non-geoeffective. With them are associated the type IV radio bursts and X-ray flares, but they are not accompanied by an increase of the SCR-intensity or by magneto-ionospheric disturbances. The absence of the large magnetic fields of spots and of the relative displacement of fields of opposite polarities promote the conservation of a closed configuration of the coronal field in such A. R. with flares.

(2) Prolonged X-ray emission (including γ-radiation in lines, Chapp et al., 1972) and the polarization of this radiation (including the post-maximum period, Tindo et al., 1973) show a definite relation of these phenomena with the eruptive phase of the flare.

(3) The relation of the IV dm and IV mB radio-bursts components with eruptive phenomena in the flare (Akinyan et al., 1971) shows that the essential changes in the coronal-field structure, with which the generation and escape of SCR

and SCP are possible, are associated with the eruptive phase of the flare.

(4) As can be seen from new observational results of SCR (Landt and Croft, 1970) within the complex magnetic field of the A. R., there is an extended ($\simeq$several hours) diffusion of low-energy SCR in the source, and their escape is determined by the degree to which the field configuration is open. This follows from the analysis of extended measurements of SCR by space vehicles, operating simultaneously.

(5) The escape of even a few discrete plasma clouds (SCP) from A. R. are observed (according to the direct coronal observations by space vehicles for hundreds (and more) minutes after the H_α-emission maximum. Long generation of SCP requires a continuous supply of chromospheric plasma to the corona, which takes place with the eruptive phenomena in the flare.

Thus, the character and intensity of its eruptive phase may be taken as an indication of the geo-effectiveness of a solar flare. This is also of importance for its further investigations.

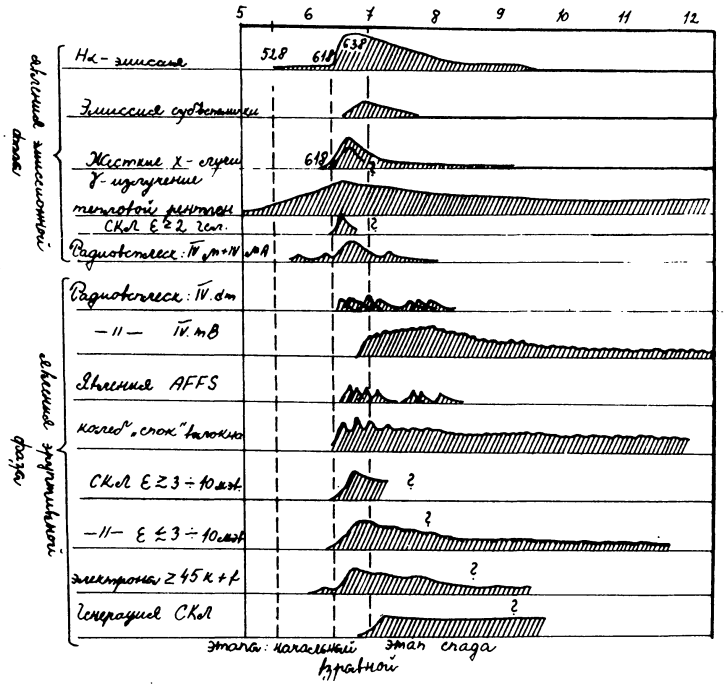

Fig. 15. The pattern of the flare phenomenon distributions for the emission and eruptive phases of the proton flare of 4.08.72.

References

AKINYAN, S. T., ISHKOV, V. N., MOGILEVSKII, E. I., BÖHME, A., FÜRSTENBERG, F., and KRÜGER, A. (1973): Proc. 7th Regional Consulations on Solar Physics. 23—29 September, 1973, Starý Smokovec.

ALTSCHULER, M. D. and TROTTER, D. E. (1973): In: Report UAG-28, Part I, 74.

BERNES, C. and KUSOFFSKY, A. U. (1973): In: Report UAG-28, Part I, 161.

BRUZEK, A. (1964): Astrophys. J., *140*, 746.

BRUZEK, A. (1969): Solar Phys., *8*, 451.

BRUZEK, A. and DEMASTUS, H. L. (1970): Solar Phys., *12*, 447.

CHAPP, E. L., FORREST, D. R., HIGBIE, P. R., SURI, A. N., TSAI, C., and DUNPHY, P. P. (1972): Nature, *241*, 333.

CHAPP, E. L., FORREST, D. R., HIGBIE, P. R., SURI, A. N., TSAI, C., and DUNPHY, P. P. (1973): In: Report UAG-28, Part II, 325.

DERE, K. P., HORAN, D. M., KREPLIN, R. W. (1973): In: Report UAG-28, Part II, 298.

DODSON, H. N. and HEDEMAN, E. R. (1970): Solar Phys., *13*, 401.

DORMAN, L. I. and MIROSHNICHENKO, L. I. (1968): Solnechnye kosmicheskie luchy. Moscow, Nauka.

FRAZIER, E. N. (1972): Solar Phys., *26*, 130.

GODOLI, G., SCINTO, V., and ZAPPALA, R. A. (1973): In: Report UAG-28, Part I, 68.

GOPASUK, S. I. (1964): Izv. KrAO, *32*, 14.

HYDER, C. L. (1966): Z. Astrophys., *63*, 78.

KOVAL, A. N. (1972): Izv. KrAO, *44*, 94.

KŘIVSKÝ, L. (1963): BAIC, *14*, No. 3.

KŘIVSKÝ, L. (1965): BAIC, *16*, 27.
KŘIVSKÝ, L. (1966): BAIC, *17*, 141.
LANDT, I. A. and CROFT, T. A. (1970): IGR, *75*, 4623.
LIVINGSTON, W. C. (1973): In: Report UAG-28, Part I, 95.
MOGILEVSKII, E. I. (1971): In: R. Howard (Ed.), Solar Magnetic Fields, IAU Symp. No. 43, Paris 1970, p. 480. Dordrecht, Reidel D. P. Co.
MOGILEVSKII, E. I. (1973): In: Report UAG-28, Part I, 139.
MOROZOV, A. I. and SOLOVEV, L. S. (1963): In: M. A. Leontovich (Ed.), Voprosy teorii plazmy. Vol. 5. Moscow, Atomizdat.
OGIR, M. B. (1967a): Izv. KrAO, *37*, 94.
OGIR, M. B. (1967b): Izv. KrAO, *36*, 69.
OGIR, M. B. (1968): Izv. KrAO, *38*, 78.
PFISTER, H. J. (1973): In: Report UAG-28, Part I, 35.
Report UAG-21, 1972.
ROY, I. R. (1972): Solar Phys., *26*, 418.
RUST, D. M. (1973): AFCRL-TR-73-0221, Environmental Res. Papers No. 440, SacPeak, Obs.
SEVERNY, A. B. (1964a): Ann. Rev. Astron. Astrophys., *2*, 636.
SEVERNY, A. B. (1964b): Izv. KrAO, *31*, 159.
SITNIK, G. F., KIRYUKHINA, A. I., MITROPOLSKAYA, O. N., NIKULIN, I. F., PORFIRIEVA, G. A., PROKUDINA, V. S., POSCHINA, E. M., KHLISTOV, A. I., KHROMOVA, T. P., and YAKULINA (1973): In: Report UAG-28, Part I, 103.
SLONIM, U. M. (1969): Astron. J., *140*, 746.
SLONIM, U. M. (1970): Doctor Thesis, 570, 697.
SOLOVEV, L. S. and SHAFRANOV, V. D. (1967): In: M. A. Leontovich (Ed.), Voprosy teorii plasmy. Vol. 5. Moscow, Atomizdat.
SOLOVEV, A. A. (1971): Soln. Dannye, No. 11, 90.
STURROCK, A. P. (1966): In: A. P. Sturrock (Ed.), Plasma Astrophys. Proc. Int. School of Physics E. Fermi, Course 39. New York, Academic Press.
STURROCK, A. P. (1968): In: K. O. Kiepenheuer (Ed.), Structure and Development of Solar Active Regions, p. 471. IAU Symp. No. 35, Budapest, 1967. Dordrecht, Reidel D. P. Co.
STURROCK, A. P. (1972): In: McIntosh (Ed.), Progress in Astronautics and Aeronautics, 30, p. 163. Cambridge, Dryer Mit. Press.
Symposium on the July 1959 Event and Associated Phenomena, Helsinki, July 1960. Paris, Inn. 18 Inst. Geophys. Nat.
SYROVATSKII, S. I. (1970): In: Solnechno-zemnaya fizika, Vol. 3, 106.
TINDO, I. P., MANDELSTAM, S. L., and SHURYGIN, A. I. (1963): Further polarization measurements of solar flare X-ray emission. Preprint No. 73, P. N. Lebedev Phys. Inst., Moscow.
ZIRIN, H. and TANAKA, K. (1973): In: Report UAG-28, Part I, 121.
ZVEREVA, A. M. and SEVERNY, A. B. (1970): Izv. KrAO, *41—42*, 97.

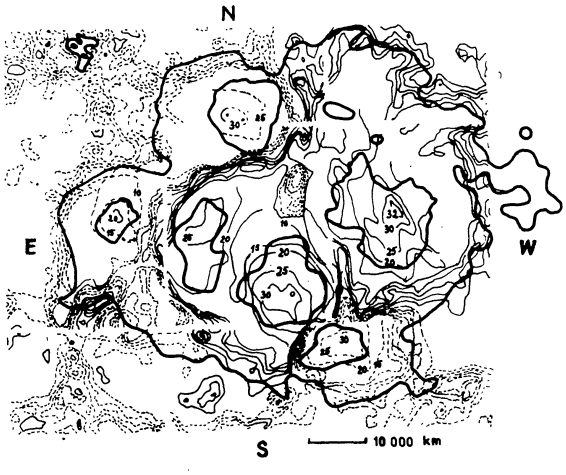

Fig. 3. (a) The chart of magnetic field in group 223 (331). Isolines: — of N-polarity, – – – of S-polarity. Solid line represents the contours of the spot umbra. Isolines field values are in hundreds of Gauss. (b) The pattern of location of umbrae of different polarities in the group. . . . . corresponds to $H_{||} = 0$. The flare ribbons and filaments are marked with contours.

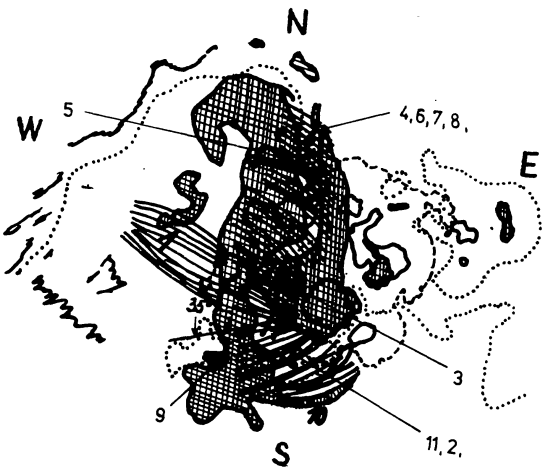

Fig. 10. The pattern of location of the observed AFFS.